REMOTE SENS. ENVIRON. 31:105–120 (1990)

Three Methods for the Absolute Calibration of the NOAA AVHRR Sensors In-Flight

P. M. Teillet, P. N. Slater, Y. Ding, and R. P. Santer†*

Optical Sciences Center, University of Arizona, Tucson

R. D. Jackson and M. S. Moran

U.S. Department of Agriculture, U.S. Water Conservation Laboratory, Phoenix

Three different approaches are described for the absolute radiometric calibration of the two reflective channels of the NOAA AVHRR sensors. Method 1 relies on field measurements and refers to another calibrated satellite sensor that acquired high-resolution imagery on the same day as the AVHRR overpass. Method 2 makes no reference to another sensor and is essentially an extension of the reflectance-based calibration method developed at White Sands for the in-orbit calibration of Landsat TM and SPOT HRV data. Method 3 achieves a calibration by reference to another satellite sensor, but it differs significantly from the first approach in that no ground reflectance and atmospheric measurements are needed on overpass day. Calibration results have been obtained using these methods for seven NOAA-9 AVHRR images and for four NOAA-10 AVHRR images. A significant degradation in NOAA-9 AVHRR responsivity has occurred since the prelaunch calibration and with time since launch. The responsivity of the NOAA-10 AVHRR has also degraded significantly compared to the prelaunch calibration. The suitabilities of using Method 2 with the Rogers (dry) Lake site in California and using Methods 1 and 3 at White Sands are discussed. The results for Method 3, which requires no field measurements and makes use of a simplified atmospheric model, are very promising, implying that a reasonable in-orbit calibration of satellite sensors may be relatively straightforward.

INTRODUCTION

Image data from the Advanced Very High Resolution Radiometer (AVHRR), flown on the NOAA TIROS-N series of operational satellites, have become an important source of information for monitoring vegetation conditions on regional and global scales (Tucker et al., 1984; Brown et al., 1982). Changes due to phenological development or varying vegetation condition can be monitored, provided that digital image counts can be related to

Address correspondence to Dr. P. M. Teillet, Canada Centre for Remote Sensing, 2464 Sheffield Rd., Ottawa, ON, Canada K1A 0Y7.

*On leave from the Canada Centre for Remote Sensing, Ottawa, Ontario, Canada K1A 0Y7.

†On leave from the Laboratoire d'Optique Atmosphérique, Université des Sciences et Techniques de Lille, 59655 Villeneuve d'Ascq Cédex, France.

Received 15 September 1989; revised 15 March 1990.

physical units such as radiance. Although AVHRR sensors are calibrated prior to launch, there is no proper on-board capability for assessing post-launch changes in absolute calibration for the visible and near-infrared spectral Channels 1 and 2. Therefore, a number of methods have been investigated with a view to providing in-orbit calibration.

Although they are necessarily less precise, some calibration methods require no additional measurements in order to achieve a multitemporal comparison. One approach is to select water bodies and forested areas near nadir and assume that they have the same reflectance from day to day throughout most of the vegetation development period (Manore and Brown, 1986). The reflectance of forested areas (both coniferous and deciduous) is roughly constant throughout this period in the red and near-infrared spectral regions. Hence, average values from forest and dark water pixels in AVHRR Channels 1 and 2 are used to standardize the imagery. In the same vein, dark counts from space views and the White Sands National Monument area in New Mexico have been used as calibration targets by Frouin and Gautier (1987). Assuming a standard value for the reflectance of the dunes area at White Sands, a radiative transfer code is invoked to predict radiance at satellite altitude, assuming standard atmospheric conditions. This radiance value and the corresponding digital image counts provide the calibration.

Several other calibration methods requiring additional data acquisition have been developed. One approach being used is to fly a well-calibrated spectroradiometer operating in the 425–1000 nm region over White Sands (Abel et al., 1988; Smith et al., 1989). The U-2 flight at 19 km altitude is timed to coincide with the satellite overpass and the viewing geometry is arranged to match that of the AVHRR sensor. An integrating sphere is used to calibrate the aircraft instrument before and after each flight. Another approach uses a ground radiometer to measure cloud radiance on an overcast day and a delta-Eddington cloud layer model to infer the irradiance incident on the cloud top images by the AVHRR (Justus, 1988). Alternatively, a direct cloud scene intercomparison can be made between the sensor to be calibrated and another calibrated sensor. Some of these methods have also been used to update the calibration of the GOES VISSR sensors. A number of other indirect calibration methods involving desert and ocean test areas are being studied, but little has been published on them as yet.

In this paper, three different approaches are described for the absolute radiometric calibration of the two reflective channels of the NOAA-9 and NOAA-10 AVHRR sensors. Method 1 relies on field measurements and data from another calibrated satellite sensor that acquired high-resolution imagery on or near the day of the AVHRR overpass. Method 2 makes no reference to another sensor and is essentially an extension of the reflectance-based calibration method developed at White Sands for the in-orbit calibration of Landsat Thematic Mapper (TM) and SPOT High Resolution Visible (HRV) data (Slater et al., 1987). Method 3 achieves a calibration by reference to another satellite sensor, but it differs significantly from the first approach in that no ground reflectance and atmospheric measurements are needed on overpass day. Calibration results have been obtained using these methods for seven NOAA-9 AVHRR images and for four NOAA-10 AVHRR images.

PRELAUNCH CALIBRATION INFORMATION

Although prelaunch calibration of the reflective AVHRR channels involved a large integrating sphere equipped with quartz lamps, it is generally provided to users in terms of coefficients based on albedo versus radiometer output (Lauritson et al., 1979; Kidwell, 1986). These coefficients are listed in a valuable set of articles by Price on calibration information and other key parameters for the major earth-viewing satellite sensors (Price, 1987; 1988a, b).

The radiance calibration coefficients have been reworked by NASA for the NOAA-9 and NOAA-10 AVHRR sensors, but they have been slow to reach the literature. The prelaunch radiance gains given in Table 1 are based on a linear regression of AVHRR sensor output as a function of integrating sphere radiance. These values correspond to the multiplicative gain coefficient a in the expression

$$D = a \times L + b, \tag{1}$$

where L = radiance and D = digital counts recorded by the instrument. The coefficients of determination obtained from linear regressions in-

Table 1. AVHRR Prelaunch Calibration Coefficients, Based on a Linear Regression of Integrating Sphere Radiance versus Digital Output in Counts from the Sensor[a]

	Gain Coefficient (counts / radiance)	*Offset Coefficient (counts)*
NOAA-9 AVHRR		
Channel 1	1.907	37.7
Channel 2	3.043	40.3
NOAA-10 AVHRR		
Channel 1	1.955	35.3
Channel 2	2.895	33.8

[a]Radiance is in units of W m^{-2} sr^{-1} μm^{-1}.

dicate that both NOAA-9 and NOAA-10 AVHRRs have a very linear response. Markham (unpublished, 1988) has tabulated space responses for NOAA-9 and NOAA-10 (Table 2). These values correspond to the additive offset coefficient b in Eq. (1). Unlike the radiance gain coefficients, the offset counts have generally not changed much since launch.

METHODS

Method 1: Ground and Atmospheric Measurements and Reference to Another Calibrated Satellite Sensor (Fig. 1)

Ground-based reflectance measurements can be made over terrain areas corresponding to numerous Landsat TM or SPOTHRV pixels, but such measurements become impractical for the calibration of the AVHRR image data with pixel dimensions of 1.1 km × 1.1 km or greater. An alternative is to acquire AVHRR imagery of White Sands on the same day that a TM or HRV calibration has been carried out on the basis of ground reflectance factor and atmospheric measurements at Chuck Site in the alkali-flat region of White Sands. The methodology then takes advantage of the accurate calibration results for TM bands 3 and 4 or HRV bands 2 and 3 to effect a calibration of AVHRR Channels 1 and 2. A reflectively uniform area corresponding to one or more AVHRR pixels is selected in the alkali-flat region and average digital counts are extracted for these AVHRR pixels and for pixels from the matching area in the TM or HRV imagery. With the help of radiative transfer computations and bidirectional reflectance data for the gypsum surface at White Sands, radiance at the entrance aperture of the AVHRR sensor is predicted. The analysis takes into account differences in spectral response, sun angle, and viewing geometry between the TM or HRV and AVHRR data acquisitions.

Method 2: Ground and Atmospheric Measurements with No Reference to Another Sensor (Fig. 2)

The second approach is based on detailed ground and atmospheric measurements near the time of AVHRR overpass. It necessarily assumes that the measured surface reflectances are representative of the whole AVHRR pixel. The availability of aircraft data can assist in the selection of an appropriately uniform area. Although this method is less precise than the first, it has the distinct advantage of not requiring nearly coincident data acquisition by two imaging sensors.

Method 3: No Ground and Atmospheric Measurements but Reference to Another Sensor (Fig. 1)

This approach achieves a calibration of the first two AVHRR channels by reference to another

Table 2. Digital Offsets in Counts for the NOAA-9 and NOAA-10 AVHRR Sensors from Markham (unpublished, 1988)[a]

	NOAA-9 AVHRR		*NOAA-10 AVHRR*	
Date	*Channel 1*	*Channel 2*	*Channel 1*	*Channel 2*
1978 (prelaunch)	—	—	35.3	33.8
1980 (prelaunch)	37.7	40.3	—	—
February 1985	38.0	39.9	—	—
February 1986	37.9	39.3	—	—
February 1987	37.8	39.1	36.9	37.6
February 1988	37.8	39.0	36.1	36.1

[a]Prelaunch values are based on a linear regression of sensor output as a function of integrating sphere radiance and in-flight values are based on responses to space views.

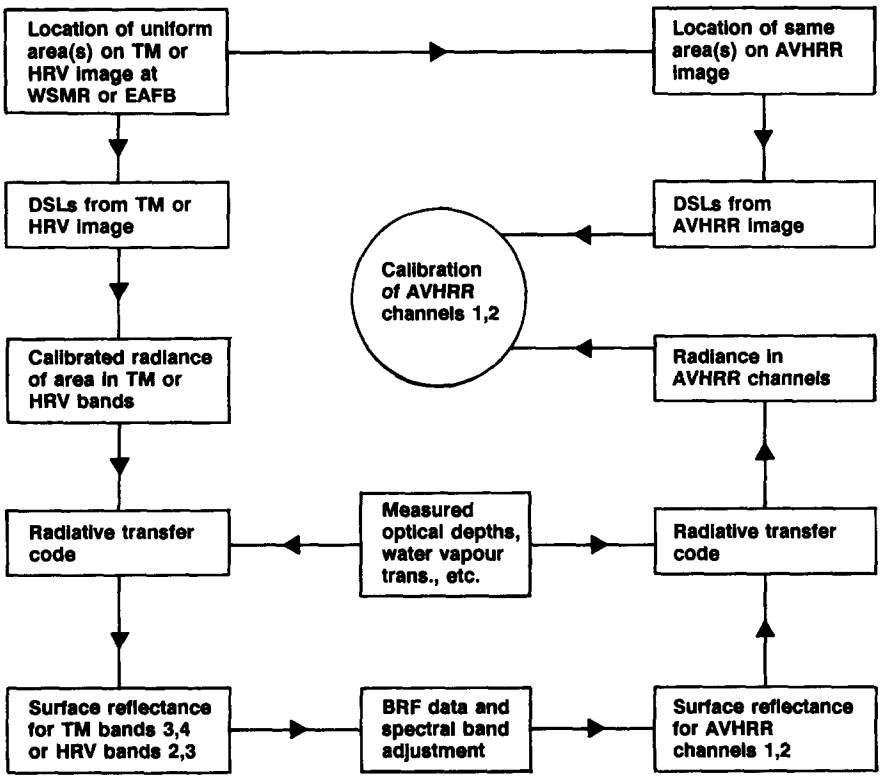

Figure 1. "Method 1" calibration approach: ground and atmospheric measurements and reference to another calibrated sensor. The "Method 3" calibration approach is based on reference to another calibrated sensor but without the need for ground and atmospheric measurements. In that case, the BRF data are historical, and the optical depths are derived from a standard mid-latitude, continental atmospheric model. In the figure, DSL = digital signal level, BRF = bidirectional reflectance factor, TM = Thematic Mapper, HRV = High Resolution Visible, WSMR = White Sands Missile Range, and EAFB = Edwards Air Force Base.

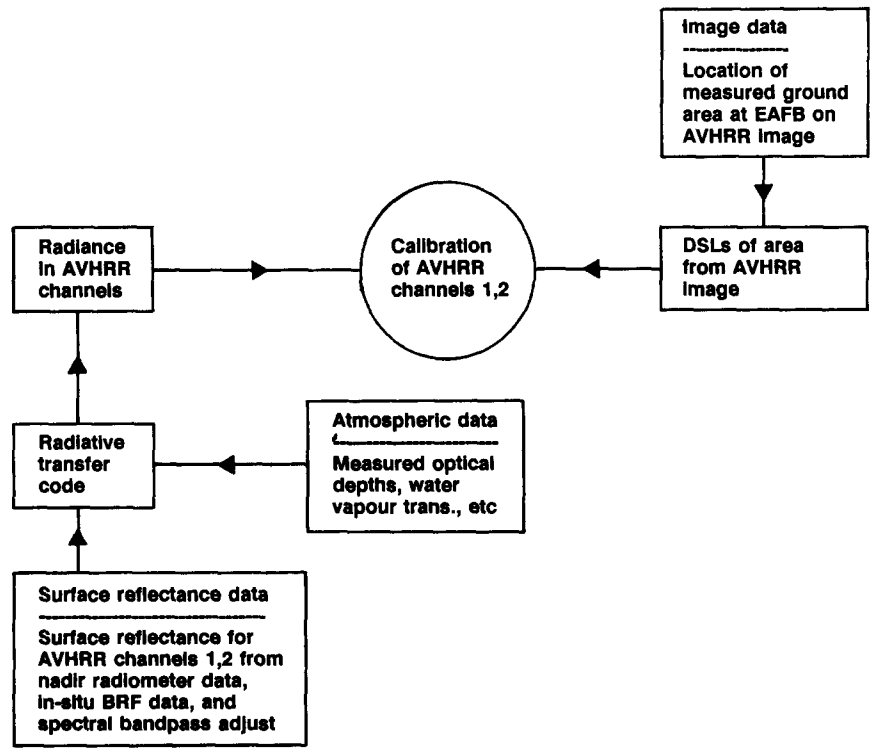

Figure 2. "Method 2" calibration approach: ground and atmospheric measurements without reference to another sensor.

satellite sensor such as the TM or HRV on the same day. However, it differs significantly in that no ground and atmospheric measurements on the overpass day are needed. Instead, a standard data set of atmospheric conditions is assumed to approximate the actual atmosphere and historical bidirectional reflectance data are used to adjust for differences in illumination and viewing geometries. The atmospheric parameters are first used to estimate surface reflectance from the TM or HRV imagery and then the same atmospheric parameters are used to predict radiance at the AVHRR sensor from that surface reflectance (suitably adjusted for bidirectional effects and spectral bandpass differences). Because of this two-way use of the atmospheric model, errors introduced in one direction will be compensated to some extent in the reverse direction so that reasonable calibration results may be obtained, provided that the procedure is not overly sensitive to the choice of atmospheric model. If viable, this approach will be valuable because it will facilitate in-orbit sensor calibration without the complexity and expense of field measurements.

NOAA-9 AND NOAA-10 AVHRR DATA SETS

The methods described in the previous section have been applied to several data sets involving NOAA-9 and NOAA-10 AVHRR imagery. The principal characteristics of these two sensor systems are listed in Table 3. As indicated in the table, prelaunch radiometric calibrations were performed many years prior to launch.

The collection of data sets involving ground-based measurements and/or same-day coverage of a test area by more than one satellite sensor is difficult to accomplish. The logistics and expense of field measurement campaigns as well as ever-present limitations due to weather severely reduce the number of data sets suitable for calibration work. An additional constraint in the case of AVHRR coverage of a given site is the possibility of large off-nadir view angles, which are not used if they exceed 40–45°. Nevertheless, several AVHRR data sets have been acquired (Table 4) over the last few years during calibration experiments at White Sands, New Mexico and at the Rogers (dry) Lake at Edwards Air Force Base (EAFB) in California. The work at EAFB has been concerned with calibration of airborne sensors and so there is no reference to another satellite sensor for that site (Method 2). At the White Sands Missle Range (WSMR), the main efforts have been directed towards in-flight calibration of the Landsat TM and SPOT HRV sensors (Slater et al., 1987; Begni et al., 1986). Hence, TM or HRV image data are used as the reference in Method 1 and Method 3 analyses. Calibration results have been obtained for seven NOAA-9 AVHRR cases 28 August 1985; 14 October 1986; 4 May 1987; 5 May 1987; 8 February 1988; 9 February 1988; 10 February 1988) and for four NOAA-10 AVHRR

Table 3. Principal Characteristics of the NOAA-9 and NOAA-10 AVHRR Sensor Systems[a]

	NOAA-9 AVHRR	*NOAA-10 AVHRR*
Prelaunch calibration	approx. February 1980	approx. March 1977
Launch date	December 1984	September 1986
Orbit	sun-synchronous ascending node (day)	sun-synchronous descending node (day)
Equatorial crossing	14:30 (approximate)	07:30 (approximate)
Nadir resolution	1.1 km	1.1 km
Scan angle range	±55.4°	±55.4°
Spectral bands (μm)	Ch. 1 (0.58–0.68)	Ch. 1 (0.58–0.68)
	Ch. 2 (0.725–1.1)	Ch. 2 (0.725–1.1)
	Ch. 3 (3.55–3.93)	Ch. 3 (3.55–3.93)
	Ch. 4 (10.3–11.3)	Ch. 4 (10.3–11.3)
	Ch. 5 (11.5–12.5)	
Quantization	10 bit	10 bit

[a]The indicated spectral bandpass limits are nominal values; the spectral response profiles of the two sensors actually differ somewhat.

cases (27 March 1987; 17 July 1987; 8 February 1988; 9 February 1988).

ANALYSIS PROCEDURES

Method 1 Analysis for NOAA-9 AVHRR on 28 August 1985 at WSMR

A geometric registration procedure was used to match the relevant portions of the TM and AVHRR images of White Sands. From the superimposed images, a relatively uniform area of two by two AVHRR pixels was selected in the alkali-flat region. The digital counts for this area and for the corresponding area in the TM imagery were extracted and averaged.

In order to relate the TM radiance values (corresponding to the aforementioned TM digital counts for the AVHRR test area) to ground reflectance factors, a series of atmospheric model computations were carried out using the Herman radiative transfer code (Herman and Browning, 1975) and ground-based measurements of Rayleigh and aerosol optical depths. The result of this step is a set of surface reflectance factors in the TM band over a much larger area than could be measured using ground-based techniques.

At the NOAA-9 satellite overpass time of 21:27 Coordinated Universal Time (UTC), the solar zenith angle was 39.85°, whereas, at the Landsat-5 satellite overpass time of 17:08 UTC, the solar zenith angle was 35.95°. Moreover, the off-nadir view angle was 23.6° for the AVHRR sensor and about 1° for the TM sensor. Thus, in order to obtain values relevant to the AVHRR conditions, corrections were applied to the TM Bands 3 and 4 reflectance factors on the basis of bidirectional reflectance (BRF) measurements made for the gypsum surface at a variety of solar zenith angles at White Sands on 15 March 1986. The reflectance factors were further adjusted to the central wavelengths of AVHRR Channels 1 and 2. The combined effect of the BRF and wavelength corrections is typically on the order of 3% for the White Sands data.

Atmospheric parameters and surface reflectances for the two AVHRR channels were then input to the Herman radiative transfer code for the return pass through the atmosphere. The result is predicted radiance at the entrance aperture of the AVHRR sensor in each channel. Both for this step and the earlier pass down through the atmosphere for TM, the French "5-S" atmospheric radiative transfer program (Tanré et al., 1985) was run to obtain the total gaseous transmittance for four cases (H_2O, O_3, CO_2, and O_2).

Method 2 Analysis for NOAA-9 AVHRR on Three Dates in EAFB

With no reference to another imaging sensor, the Method 2 calibration approach relies on ground-based measurements of atmospheric conditions and surface reflectance made at the site on the day of an overpass with the techniques used at White Sands (Slater et al., 1987). Solar radiometer data

Table 4. NOAA-9 and NOAA-10 AVHRR Data Sets[a]

Date	*Site*	*Reference Sensor*
	NOAA-9 AVHRR Data Sets	
1985.08.28 (260)	WSMR	TM
1986.10.14 (672)	EAFB	—
1987.05.04 (874)	EAFB	—
1987.05.05 (875)	EAFB	—
1988.02.08 (1155)	WSMR	TM, HRV from 1988.02.10
1988.02.09 (1156)	WSMR	TM, HRV from 1988.02.10
1988.02.10 (1157)	WSMR	TM, HRV
	NOAA-10 AVHRR Data Sets	
1987.03.27 (192)	WSMR	TM
1987.07.17 (305)	WSMR	HRV
1988.02.08 (511)	WSMR	TM, HRV from 1988.02.10
1988.02.09 (512)	WSMR	TM, HRV from 1988.02.10

[a]The bracketed number after the date refers to the number of days since launch. WSMR is the White Sands Missile Range in New Mexico and EAFB is Edwards Air Force Base in the Mojave Desert of California.

were acquired next to Rogers (dry) Lake at EAFB on 14 October 1986, 4 May 1987, and 5 May 1987. On 14 October and 5 May, reflectance factor measurements were made on the dry lakebed over a 320 m×80 m target area. The measured reflectance factors were acquired with nadir viewing geometry and usually not at AVHRR overpass time (and hence at a different sun angle). Thus, the reflectance factors were corrected to the sun and view angle geometries for the NOAA-9 AVHRR overpasses of EAFB on the three dates. These corrections used BRF measurements made on the dry lakebed at a variety of solar zenith angles on 5 May 1987, 6 May 1987, and 14 September 1987. Because of the non-Lambertian character of the playa surface, the BRF corrections can reach 15–20% for cases involving large off-nadir angles. A final adjustment (on the order of 1–2%) was made to the reflectance factors to correspond to the central wavelengths of AVHRR Channels 1 and 2. The use of the Herman and "5-S" codes is as described earlier in the Method 1 approach.

Bright and dark features were identified in SPOT HRV and Airborne Visible and Infrared Imaging Spectrometer (AVIRIS) imagery, acquired at other times for the EAFB area, that were also distinguishable in the AVHRR scenes. The features used for this purpose were not likely to have changed places in time and were sufficiently numerous to minimize the effect of systematic geometric distortions. The location of the ground measurement site on the dry lakebed could then be estimated visually in the AVHRR imagery using relative distances and triangulation. Digital image analysis facilities were used for this purpose. The corresponding "best estimate" digital counts were then interpolated from image values in AVHRR Channels 1 and 2.

The surface at Rogers (dry) Lake is quite flat over a wide area but its reflectance characteristics are reasonably uniform only in a limited area, roughly 1 3/4 km in the predominantly East–West direction. Thus, although that part of the dry lakebed provides a large uniform target for high-resolution sensors, it can accommodate the area of one AVHRR pixel only for off-nadir view angles less than 35° relative to vertical at ground level (the approximate pixel dimensions on the various data are listed in Table 5). Because this site is not easy to pinpoint in the AVHRR imagery, digital counts were also obtained by interpolation for locations plus or minus half a pixel away in the direction of the steepest radiance gradient.

Method 3 Analysis for NOAA-9 AVHRR on 28 August 1985 at WSMR

The data flow for this method resembles that of Method 1, but it differs considerably in nature in that ground-based measurements of atmospheric conditions and surface reflectance are not required. The atmosphere is approximated by a standard set of atmospheric conditions and the "5-S" atmospheric model is invoked as a fast code to use. Historical BRF data are used to adjust retrieved TM reflectance factors to the illumination and viewing geometries pertinent to the AVHRR overpass. In other respects, the analysis procedure is identical to Method 1.

Table 5. Sun and View Angle Geometries for the NOAA-9 and NOAA-10 AVHRR Overpasses[a]

Date	*Overpass Time (U.T.)*	*Solar Zenith (deg)*	*Solar Azimuth (deg)*	*Solar Distance (A.U.)*	*Off-Nadir View (deg)*	*View Azimuth (deg)*	*Approximate Pixel Dimensions (km)*
1985.08.28	21:27:00	39.9	242.1	1.0098	23.6	259	1.4×1.3
1986.10.14	21:46:55	53.0	221.6	0.9972	44.5	259	2.2×1.6
1987.05.04	22:29:54	40.7	252.8	1.0087	15.3	79	1.3×1.2
1987.05.05	22:19:03	38.5	250.8	1.0087	31.3	79	1.6×1.3
1987.03.27	15:15:45	62.7	107.0	0.9979	21.5	281	1.3×1.2
1987.07.17	14:46:32	59.2	83.3	1.0164	32.3	101	1.6×1.4
1988.02.08	15:11:32	76.2	118.6	0.9862	10.5	281	1.2×1.2
1988.02.08	22:22:00	64.8	229.7	0.9862	1.9	259	1.2×1.2
1988.02.09	14:49:51	80.1	115.0	0.9864	27.1	101	1.5×1.3
1988.02.09	22:11:10	62.8	227.7	0.9864	16.6	79	1.3×1.2
1988.02.10	22:00:22	60.9	225.7	0.9866	32.5	79	1.6×1.4

[a]The nadir view angles are relative to vertical at ground level and view azimuth angles are in the satellite direction from the ground location.

Table 6. Sensitivity Analysis Selections for Input to the "5-S" Code used in Method 3 Calibration Analyses

Visibility (km)	*Aerosol Model*	*Atmospheric Model*
200	continental	midlatitude summer
100	continental	midlatitude summer
50	continental	midlatitude summer
23	continental	midlatitude summer
200	maritime	tropical
100	maritime	tropical
50	maritime	tropical
23	maritime	tropical
200	continental	subarctic winter
100	continental	subarctic winter
50	continental	subarctic winter
23	continental	subarctic winter

It is of interest to test the sensitivity of Method 3 to the assumed atmospheric characteristics, such as visibility, aerosol model, and atmospheric profile (Tanré et al., 1985; McClatchey et al., 1971). The cases examined are listed in Table 6. The nominal case for the White Sands area is 100 km visibility, continental aerosols, and a midlatitude summer profile.

Method 1 and Method 3 Analyses for NOAA-10 AVHRR on 27 March 1987 at WSMR

Compared to the Method 1 and Method 3 analyses for NOAA-9 AVHRR, the only differences in the case of the NOAA-10 AVHRR concern image data manipulation. Unlike the situation with NOAA-9, the NOAA-10 AVHRR and the Landsat TM sensors acquire images from similar orbital configurations (descending orbit). Thus, no significant rotation was necessary to superimpose the two image data sets and the main factor to be dealt with was the different off-nadir viewing angles involved.

The other difference is not inherent to the NOAA-10 AVHRR sensor but rather concerns the adoption of a different procedure for selecting common areas in the TM and AVHRR scenes. The TM scene was examined on a digital image display for relatively uniform patches greater than one AVHRR pixel in extent. Ten such locations were identified, seven in the alkali-flat region for use in the actual analysis and three in the dunes area for comparison. Block averages of 45 pixles by 41 lines (corresponding to the size of one AVHRR pixel) were obtained in TM Band 3 and Band 4 image data centered in each of the 10 areas. The

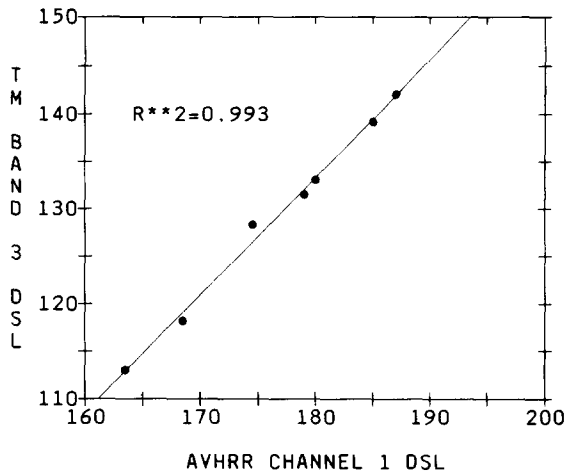

Figure 3a). Comparison of digital counts from AVHRR Channel 1 and TM Band 3 on 27 March 1987 for seven locations in the alkali-flats region at White Sands after geometric registration. The straight line is a linear regression fit.

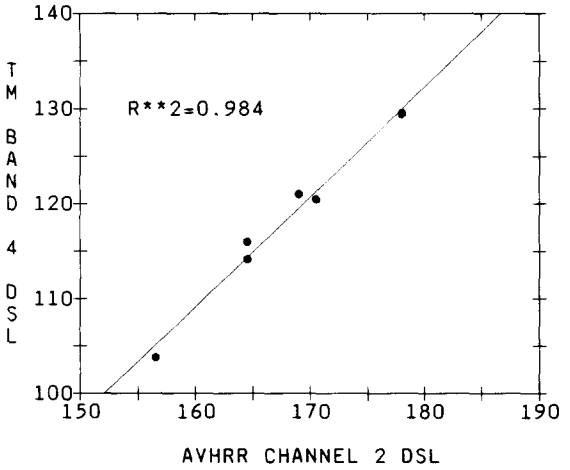

Figure 3b). Comparison of digital counts from AVHRR Channel 2 and TM Band 4 on 27, March 1987 for seven locations in the alkali-flats region at White Sands after geometric registration. Two points fall in the same place (the brightest location) and so only six points are distinguishable in the plot. The straight line is a linear regression fit.

central locations were then identified in the registered AVHRR imagery and corresponding digital counts were obtained from AVHRR Channels 1 and 2. Because each of the uniform images patches was well over one AVHRR pixel in extent and only one AVHRR sample was taken from each such area, problems due to misregistration were minimized. Figure 3 shows that there is some merit to this approach. It plots digital counts from AVHRR Channel 1 against TM Band 3 and AVHRR Channel 2 against TM Band 4 after geometric registration, with linear regressions yielding coefficients of

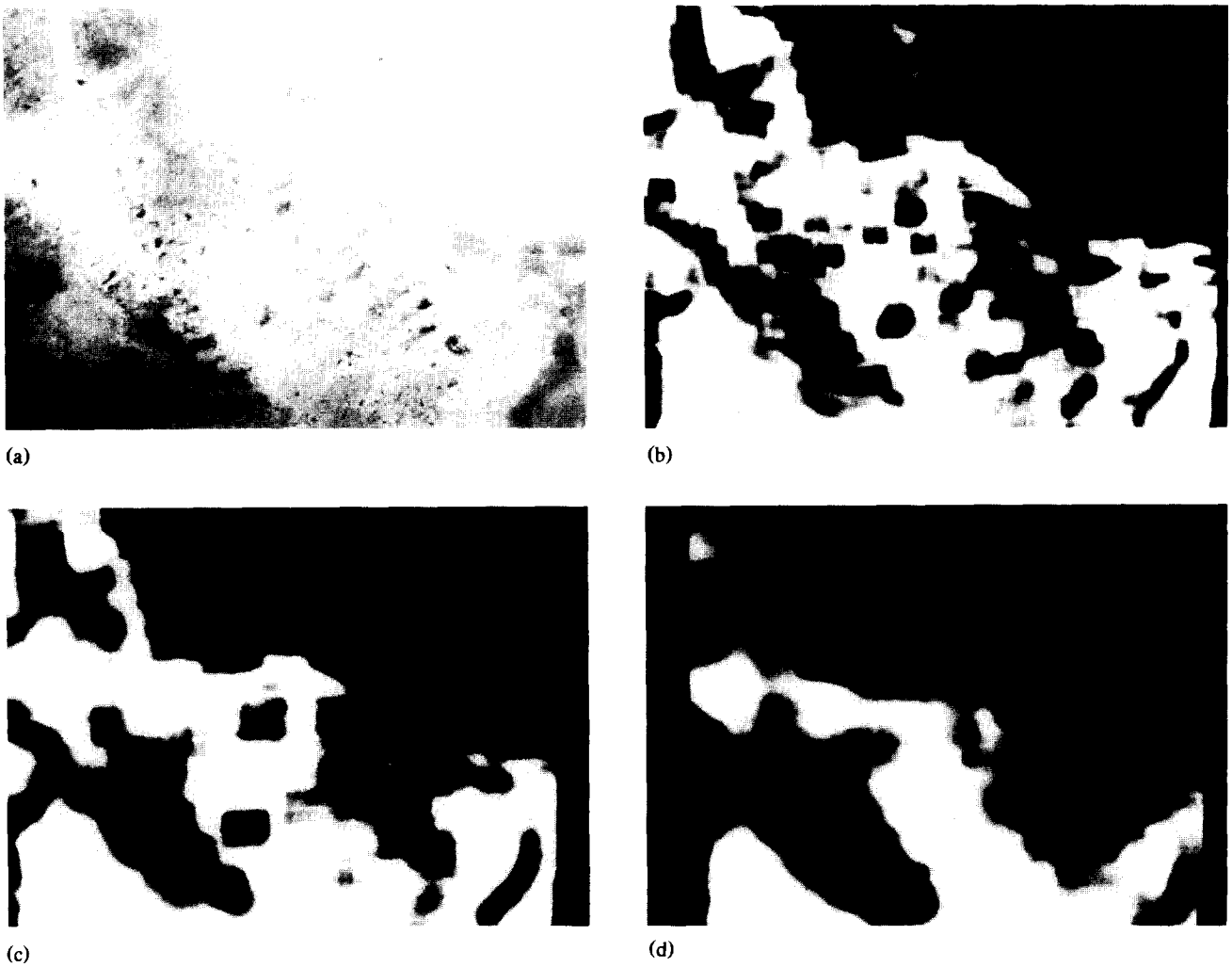

Figure 4. White Sands area in a) TM Band 3 and the results of a variance operator applied to that band for scanning window sizes of b) 21 pixels by 21 lines, c) 41 pixels by 41 lines, and d) 81 pixels by 81 lines. The variance operator is defined so that the brighter the digital value is, the more uniform the image was in the window.

determination of 0.993 and 0.984, respectively.

Method 1 Analysis for NOAA-9 and NOAA-10 AVHRR in February 1988 at WSMR

Ground-based measurements of surface reflectance and solar extinction were made at White Sands on 8, 9, and 10 February 1988. AVHRR coverage consisted of afternoon imagery from NOAA-9 on all three days and early morning imagery from NOAA-10 on the first two days. Landsat-5 TM and SPOT HRV images were acquired over the site on 10 February. Method 1 calibration results have been obtained for all five AVHRR cases using the calibrated TM scene as the reference. The surface reflectance values obtained over extended areas from the TM data were adjusted to suit the two earlier days with the help of the surface reflectances measured on all three days at Chuck Site. This adjustment necessarily assumes that the relationship between reflectances at Chuck Site and in the alkali-flats at large remained reasonably constant on all three days.

Compared to the Method 1 analyses for earlier data sets, the only difference in the case of the February 1988 data sets concerns image data manipulation. A more objective procedure for selecting common areas in the TM (or HRV) and AVHRR scenes was implemented. A variance window operator was applied to TM Band 3 and to TM Band 4 in order to help identify uniform regions for use in the AVHRR calibration. The operator is defined as $(100 - \text{variance}) \times 255/100$, where the variance is obtained from the digital image values in a

specified window. The window is scanned across the image in question, with the central pixel replaced by the digital value computed by the operator. The resulting variance image has high digital values wherever the variance in the image is low, which is the situation to be identified. Window sizes of n pixels by n lines with $n = 21$, 41, and 81 were used for TM Bands 3 and 4. The size of an AVHRR pixel near nadir is on the order of 41 pixels by 41 lines in a TM image. Examination of the variance images from both TM Bands 3 and 4 then allowed a more objective selection of relatively uniform patches greater than one AVHRR pixel in extent. Results of the use of the variance operator for different window sizes are shown in Figure 4.

For the February scenes, fewer uniform patches were found in TM Band 4, probably because of the considerable amount of standing water present at WSMR at that time and the darkness of water in that band in contrast to the bright gypsum surface. Only those locations identified in both TM Bands 3 and 4 were used in further analysis. A few tests also indicated that the visual selection approach used on earlier data sets compared favorably with the more objective method. Nevertheless, the newer approach provides a more thorough search for locations and is particularly helpful when the surface in the alkali-flat region is more heterogeneous than usual (as was the case in February 1988).

NOAA-9 AVHRR CALIBRATION RESULTS

Absolute calibration coefficients for the reflective channels of the NOAA-9 AVHRR are listed in Table 7 and portrayed as a function of time in Figures 5a) and 5b). It is evident that the sensor's responsivity has degraded significantly with time, with the greater change occurring in Channel 2. That the estimated gain coefficients in October 1986 should be a lot lower than for later dates is largely due to the difficulty in making a precise BRF correction for the earlier date when the off-nadir view angle was nearly 45°, but also partly due to the problem of having a 2.2 km pixel dimension in the scan line direction, which exceeds the size of the uniform reflectance patch at EAFB. The results for 4 and 5 May 1987 are reasonably consistent. Although the same surface reflectance measurements were used for both days since no reflectance measurements were made on 4 May, different atmospheric parameters were used and the off-nadir view angles differed considerably (Table 3). The results for the three February dates are also reasonably consistent. The error bars in Figure 5 are based on the analysis outlined in Table 8, indicating a conservative or worst-case estimate of uncertainty on the order of seven to eight percent.

Method 3 and Method 1 calibration results on 28 August 1985 are compared in Table 9. If the atmospheric parameters at White Sands were unknown, the standard conditions would be assumed to be a midlatitude summer profile with continental aerosols and a visibility of 100 km. The difference between the two methods in that case is 1.1% in Channel 1 and 3.0% in Channel 2. There appears to be very little sensitivity to the assumed visibility and a slight sensitivity to a change to a moister atmosphere (tropical) with maritime aerosols. The greatest effect in this regard occurred in Channel 2 with a change to a drier atmosphere (subarctic winter). Notable differences between the two methods also arise if no corrections are made for sun angles, view angle, and wavelength differences between the TM and AVHRR conditions.

Table 7. NOAA-9 AVHRR Radiometric Calibration Results[a]

Date	*Method*	*Channel 1 Gain*	*Channel 2 Gain*
Prelaunch		1.907	3.043
1985.08.28	1	1.83	2.57
1986.10.14	2	1.37 (1.47, 1.32)	2.06 (2.21, 1.97)
1987.05.04	2	1.49 (1.55, 1.44)	2.25 (2.34, 2.17)
1987.05.05	2	1.51 (1.60, 1.43)	2.30 (2.43, 2.17)
1988.02.08	1	1.40	2.11
1988.02.09	1	1.38	2.15
1988.02.10	1	1.42	2.23

[a]For Method 2 at EAFB, results are given in parentheses for locations plus or minus half a pixel away in the scan direction. Gain coefficients are in units of counts/(W m^{-2} sr^{-1} μm^{-1}).

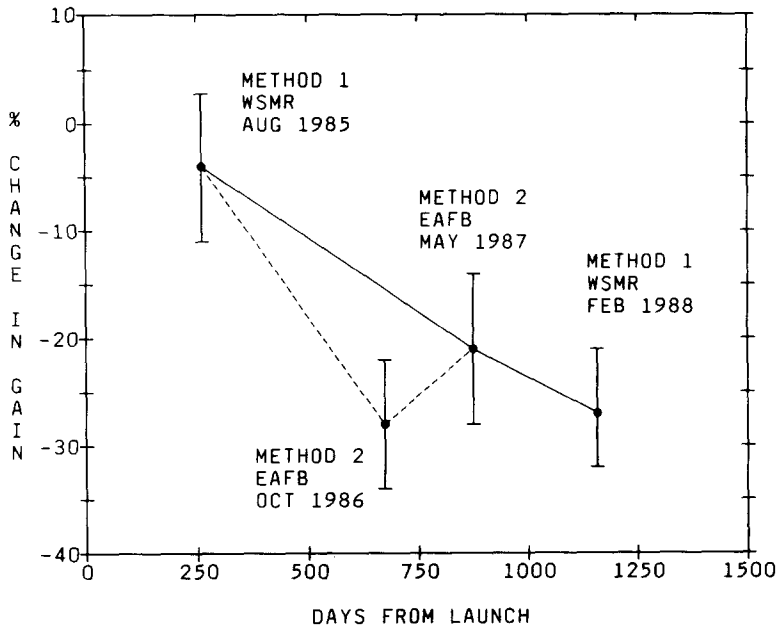

Figure 5a). NOAA-9 AVHRR Channel 1 calibration results expressed as percent change in gain as a function of time. The May 1987 result is an average from 4 and 5 May. The February 1988 result is an average from 8, 9, and 10 February.

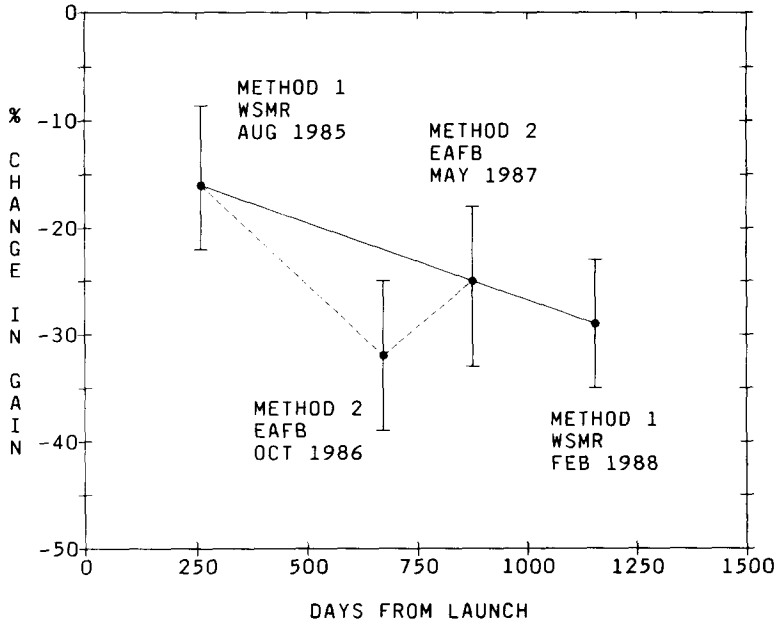

Figure 5b). NOAA-9 AVHRR Channel 2 calibration results expressed as percent change in gain as a function of time. The May 1987 result is an average from 4 and 5 May. The February 1988 result is an average from 8, 9, and 10 February.

Table 8. Conservative or Worst-Case Estimate of Uncertainty in Predicted AVHRR Gain

	Method 1 at WSMR	*Method 2 at EAFB*
Registration of TM/HRV and AVHRR data	±1%	N/A
AVHRR pixel phasing with respect to ground site	N/A	±6%
Calibration of TM/HRV data	±5% (less for TM)	N/A
Surface reflectance measurements	±1%	±1%
Atmospheric measurements and modeling	±4%	±3%
BRF adjustment	less than ±1%	±6%
Spectral bandpass adjustment	±1% (±4% in ch. 2)	±1% (±4% in ch. 2)
Uncertainty from use of several pixel sites	±2% (±3% in ch. 2)	N/A
Root sum square	±7% (±8% in ch. 2)	±9% (±10% in ch. 2)

Table 9. Method 3 Calibration Results for NOAA-9 for 28 August 1985[a]

Visibility (km)	*Atmospheric Profile*	*Aerosol Model*	*Channel 1 Gain*	*Difference from Method 1*	*Channel 2 Gain*	*Difference from Method 1*
200	M.L.S.	Cont.	1.85	+1.1%	2.65	+3.0%
100	M.L.S.	Cont.	1.85	+1.1%	2.65	+3.0%
50	M.L.S.	Cont.	1.85	+1.1%	2.65	+3.0%
23	M.L.S.	Cont.	1.86	+1.6%	2.65	+3.0%
200	Trop.	Marit.	1.84	+0.54%	2.67	+3.7%
100	Trop.	Marit.	1.83	0.%	2.67	+3.7%
50	Trop.	Marit.	1.83	0.%	2.67	+3.7%
23	Trop.	Marit.	1.82	−0.65%	2.65	+3.0%
200	S.A.W.	Cont.	1.87	+2.1%	2.53	−1.6%
100	S.A.W.	Cont.	1.87	+2.1%	2.53	−1.6%
50	S.A.W.	Cont.	1.87	+2.1%	2.53	−1.6%
23	S.A.W.	Cont.	1.88	+2.7%	2.53	−1.6%
With no BRF and no λ adjustment:						
200	M.L.S.	Cont.	1.87	+2.1%	2.74	+6.2%
50	M.L.S.	Cont.	1.88	+2.7%	2.74	+6.2%
"Matched"	M.L.S.	Cont.	1.85	+1.1%	2.58	+0.39%
	Method 1 results:		1.83		2.57	
	Prelaunch values:		1.907		3.043	

[a] M.L.S. = midlatitude summer, S.A.W. = subarctic winter, Trop. = tropical; Cont. = continental; Marit. = maritimes. "Matched" refers to 5S runs using measured aerosol and Rayleigh optical depth values. Gain coefficients are in units of counts/(W m^{-2} sr^{-1} μm^{-1}).

NOAA-10 AVHRR CALIBRATION RESULTS

Absolute calibration coefficients based on Method 1 for the reflective channels of the NOAA-10 AVHRR on 27 March 1987 are given in Table 10. Results for the dunes differ considerably from those of the alkali-flats, probably because the BRF corrections based on data acquired at Chuck Site are not applicable to the dunes area. Conversely, the consistency between results for the various alkali-flats locations indicates that the BRF corrections can be extended widely in that region of White Sands. Calibration coefficients for three dates are listed in Table 11 and portrayed as a function of time in Figure 6. As for the NOAA-9 instrument, the NOAA-10 AVHRR responsivity has degraded significantly with time and the greater change has occurred in Channel 2. The increase in gain coefficients for July 1987 has not been explained yet, although the coefficients are probably not significantly higher given the uncertainty in the method. The HRV sensor was used as the reference for that day and the drop may be related. Further work is needed to sort this problem out.

Method 3 and Method 1 calibration results for 27 March 1987 are compared in Table 12. The results for 17 July 1987 are comparable. Similarly to the case discussed in the previous section, results from the two methods are generally within a few percent of each other. The greatest difference occurs in Channel 2 if the atmosphere is assumed to be a subarctic winter model.

IMPACT OF CALIBRATION CHANGES ON VEGETATION INDICES

The calibration results indicate that the degradation in responsivity of the AVHRR sensor differs between Channel 1 and Channel 2. Therefore, it is to be expected that vegetation indices based on a ratio or a normalized difference involving AVHRR Channels 1 and 2 will be affected. A vegetation index defined as a simple difference between Channel 2 and Channel 1 will be affected by a change in calibration even if the change is the same percentage in both channels.

To illustrate the magnitude of this problem, the "5-S" atmospheric code was used to simulate vegetation indices for the NOAA-9 AVHRR spectral response profiles and a uniform vegetation target. The input conditions of "5-S" code runs are listed in Table 13. Three vegetation indices were defined as follows:

$$\text{RATIO} = D_2 / D_1, \tag{2}$$

$$\text{DIFF} = D_2 - D_1, \tag{3}$$

$$\text{NDVI} = (D_2 - D_1)/(D_2 + D_1), \tag{4}$$

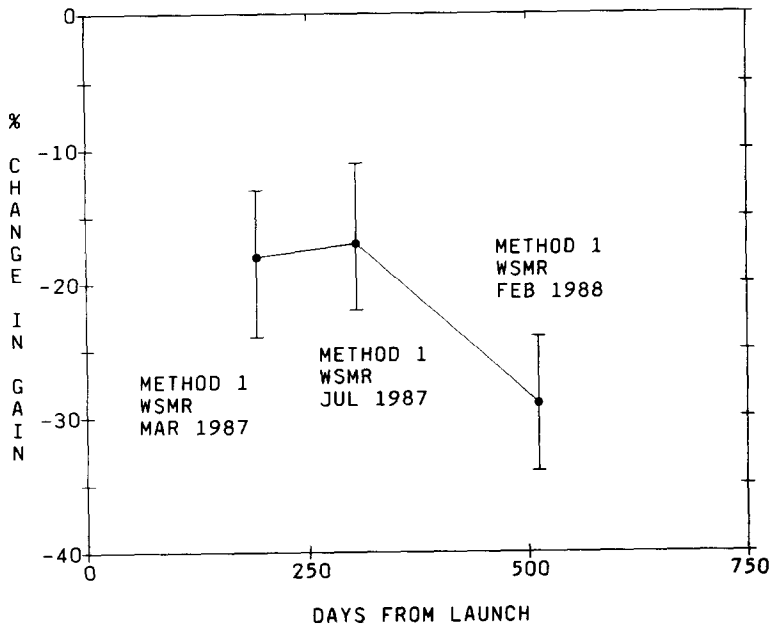

Figure 6a). NOAA-10 AVHRR Channel 1 calibration results expressed as percent change in gain as a function of time. The February 1988 result is an average from 8 and 9 February.

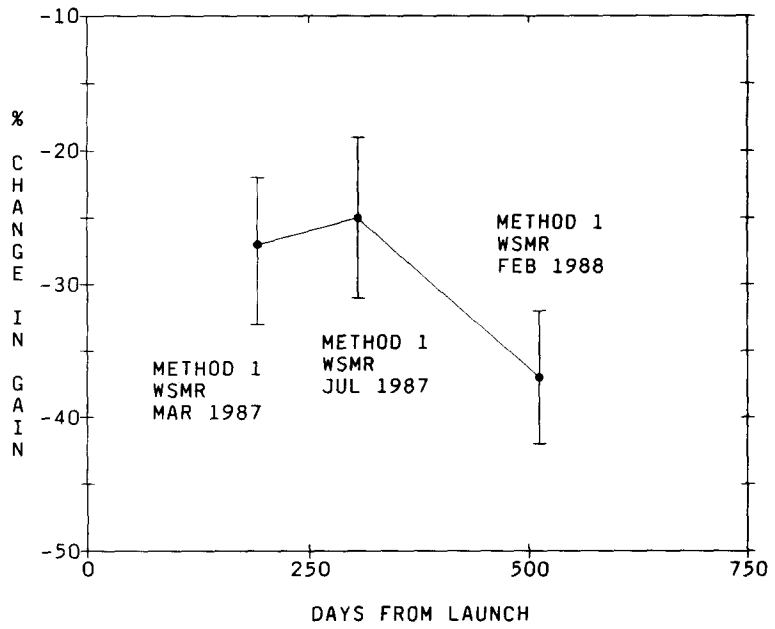

Figure 6b). NOAA-10 AVHRR Channel 2 calibration results expressed as percent change in gain as a function of time. The February 1988 result is an average from 8 and 9 February.

where D represents digital counts on a 10-bit scale and the subscript refers to the AVHRR channel number. The D values were obtained by applying the calibration gain and offset coefficients to the apparent radiance output by the "5-S" code. Different vegetation indices could then be formed with the NOAA-9 AVHRR calibration, and compared to values based on prelaunch calibration coefficients.

The results are presented in Figure 7 in terms of percent change in vegetation index as a function of time. From February 1986 to February 1988, the RATIO and NDVI values increased slightly, whereas the DIFF values decreased substantially. Thus, the key vegetation index derived from NOAA-9 AVHRR data, NDVI, will have gradually increased at the rate of about 1–2% per year, even if vegetation conditions have not actually changed. However, a significant difference in vegetation condition or land-use pattern can alter AVHRR NDVI values by 10–20% or more. Thus, the observed performance degradation will have a small

Table 10. NOAA-10 AVHRR Radiometric Calibration Results Based on Method 1 for 27 March 1987 at White Sands[a]

Location	Channel 1 Gain	Channel 2 Gain
#1	1.66	2.25
#2	1.60	2.14
#3	1.61	2.12
#4	1.61	2.16
#5	1.58	2.11
#6	1.65	2.17
#7	1.59	2.11
Mean	1.61	2.15
Std. dev.	0.030	0.050
Prelaunch	1.955	2.895
#1 (dunes)	1.45	1.96
#2 (dunes)	1.48	1.98
#3 (dunes)	1.60	2.10

[a]The first seven locations listed are in the alkali-flats region. Gain coefficients are in units of counts/(W m^{-2} sr^{-1} μm^{-1}).

Table 11. NOAA-10 AVHRR Radiometric Calibration Results[a]

Date	Reference Sensor	Channel 1 Gain	Channel 2 Gain
Prelaunch	—	1.955	2.895
1987.03.27	TM	1.60	2.10
1987.07.17	HRV	1.63	2.18
1988.02.08	TM	1.41	1.88
1988.02.09	TM	1.36	1.75

[a]Method 1 was used in all cases. Gain coefficients are in units of counts/(W m^{-2} sr^{-1} μm^{-1}).

Table 13. Input Conditions for the 5S Code Runs for Vegetation Index Comparisons

Terrain elevation	0 km
Sensor altitude	999 km
Solar zenith angle	45°
Solar azimuth angle	225°
Sensor zenith angle	35°
Sensor azimuth angle	78°
Atmospheric profile	Mid-latitude summer
Aerosol model	Continental
Visibility	23 km
Surface reflectance	Uniform vegetation
Spectral bands	NOAA-9 AVHRR Channels 1 and 2

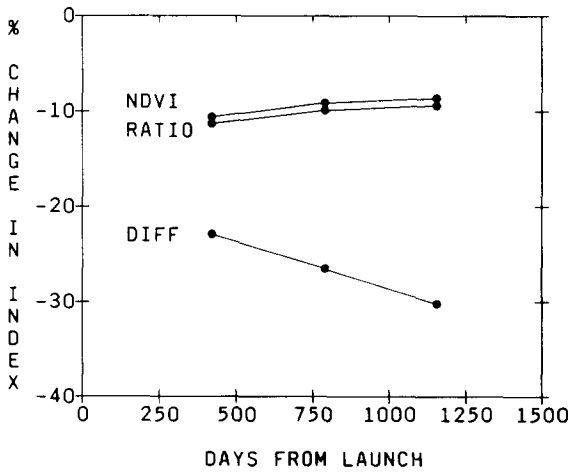

Figure 7. NOAA-9 AVHRR vegetation index changes as a function of time. RATIO, NDVI, and DIFF are defined in the text.

Table 12. Method 3 Calibration Results for NOAA-10 for 27 March 1987[a]

Visibility (km)	Atmospheric Profile	Aerosol Model	Channel 1 Gain	Difference from Method 1	Channel 2 Gain	Difference from Method 1
200	M.L.S.	Cont.	1.58	−1.3%	2.04	−3.4%
100	M.L.S.	Cont.	1.58	−1.3%	2.05	−2.9%
50	M.L.S.	Cont.	1.59	−0.63%	2.07	−1.9%
23	M.L.S.	Cont.	1.60	0.%	2.11	0.%
200	Trop.	Marit.	1.56	−2.6%	2.07	−1.9%
100	Trop.	Marit.	1.57	−1.9%	2.07	−1.9%
50	Trop.	Marit.	1.57	−1.9%	2.09	−0.96%
23	Trop.	Marit.	1.56	−2.6%	2.09	−0.96%
200	S.A.W.	Cont.	1.61	+0.62%	1.94	−8.8%
100	S.A.W.	Cont.	1.62	+1.2%	1.95	−8.2%
50	S.A.W.	Cont.	1.62	+1.2%	1.96	−7.7%
23	S.A.W.	Cont.	1.63	+1.8%	2.00	−5.5%
With no BRF and no λ adjustment:						
200	M.L.S.	Cont.	1.61	+0.62%	2.13	+0.94%
50	M.L.S.	Cont.	1.62	+1.2%	2.16	+2.3%
		Method 1 results	1.60		2.11	
		Prelaunch values:	1.955		2.895	

[a]M.L.S. = midlatitude summer, S.A.W. = subarctic winter, Trop. = tropical; Cont. = continental; Marit. = maritimes. Gain coefficients are in units of counts/(W m^{-2} sr^{-1} μm^{-1}).

effect on NDVI from year to year but should be corrected for vegetation monitoring that spans the lifetime of the sensor.

CONCLUSIONS

Significant degradations in NOAA-9 and NOAA-10 AVHRR responsivities have occurred since the prelaunch calibration and with time since launch. As of February 1988, the changes for the NOAA-9 instrument compared to prelaunch values were on the order of −27% in Channel 1 and −29% in Channel 2, and for the NOAA-10 AVHRR, the changes were −29% and −37% in Channels 1 and 2, respectively. Uncertainties in the calibration methods used to derive these results are on the order of 7–10% percent, a level of accuracy that is insufficient for many applications. On-board radiometric calibration capabilities are essential in future sensor systems. Meanwhile, the analysis of additional data sets is needed on a continuing basis to update and further characterize the degradations in AVHRR performance.

There are some limitations to the use of Method 2 with the Rogers (dry) Lake site at Edwards Air Force Base. The uniform area is limited to one AVHRR pixel (for nadir view angles less than 35° relative to vertical at ground level) and is surrounded by terrain of much brighter and much darker reflectance on either side. In addition, unlike the gypsum at White Sands, the surface is not very lambertian so that accurate BRF corrections are important. (It should also be noted that the radiative transfer codes used assume lambertian reflectance.) Method 2 using the Rogers (dry) Lake site is not likely to be able to track gain changes less than about 10%.

In both Methods 1 and 3, corrections for sun angle, view angle, and spectral differences between the higher resolution data and the AVHRR data are important, as is a good calibration of the high resolution sensor. For the data sets analyzed to date, the alkali-flats area at White Sands has proved to be quite suitable for the Method 1 and Method 3 approaches.

As far as Method 3 is concerned, results are generally within 1–3% of Method 1 for the conditions usually expected at White Sands. The method is not very sensitive to assumed visibility and hence aerosol optical depth, but it does show some sensitivity to the assumed atmospheric profile and hence water vapor, especially in Channel 2. Nevertheless, the results for Method 3, which requires no field measurements and makes use of a simplified atmospheric model, are very promising. Because the results from this approach compare favorably with the more detailed methods and are not overly sensitive to assumed atmospheric conditions, the implication is that a reasonable calibration of satellite sensors may be possible by transfer, without the necessity of making ground-based measurements. In this way, it would be relatively straightforward to monitor occasionally (and retrospectively as well) the status of AVHRR sensor radiometric responses.

The impact of changes in AVHRR calibration on the normalized difference vegetation index has been found to be small on a year-to-year basis but significant over the lifetime of the sensor.

The authors wish to thank G. Smith and B. L. Markham for their help in providing digital imagery, as well as R. Frouin, C. Whitlock, G. Vane, and M. Manore for useful discussions. Y. Mao, B. Yuan, R. J. Bartell, and S. F. Biggar assisted with aspects of the data reduction. We also wish to thank B. M. Herman for the use of his radiative transfer code and J. A. Reagan for the use of his solar radiometer. The work at the University of Arizona was supported by NASA Grants NAG5-859 and NAGW-896.

REFERENCES

Abel, P., Smith, G. R., Levin, R. H., and Jacobowitz, H. (1988), Results from aircraft measurements over White Sands, New Mexico, to calibrate the visible channels of spacecraft instruments, in *Recent Advances in Sensors, Radiometry, and Data Processing for Remote Sensing*, Proc. SPIE, Vol. 924, pp. 208–214.

Begni, G., Dinguirard, M. C., Jackson, R. D., and Slater, P. N. (1986), Absolute calibration of the SPOT-1 HRV cameras, in *Earth Remote Sensing Using the Landsat Thematic Mapper and SPOT Sensor Systems*, Proc. SPIE, Vol. 660, 66–76.

Brown, R. J., Bernier, M., Fedosejevs, G., and Skretkowica, L. (1982), NOAA AVHRR crop condition monitoring, *Can. J. Remote Sens.* 8:107–117.

Frouin, R., and Gautier, C. (1987), Calibration of NOAA-7 AVHRR, GOES-5, and GOES-6 VISSR/VAS solar channels, *Remote Sens. Environ.* 22:73–101.

Herman, B. M., and Browning, S. R. (1975), The effect of aerosols on the earth atmosphere albedo, *J. Atmos. Sci.* 32:158–165.

Justus, C. G. (1988), Calibration of satellite shortwave sensors using overcast cloudlayer targets, in *Recent Advances in Sensors, Radiometry, and Data Processing for Remote Sensing*, Proc. SPIE, Vol. 924, pp. 120–128.

Kidwell, K. B. (1986), *NOAA Polar Orbiter Data Users' Guide*, National Oceanic and Atmospheric Administration, World Weather Building, Room 100, Washington, DC.

Lauritson, L., Nelson, G. J., and Porto, F. W. (1979), Data extraction and calibration of TIROS-N/NOAA radiometers, NOAA Technical Memorandum NESS 107, National Oceanic and Atmospheric Administration, World Weather Building, Washington, DC.

Manore, M., and Brown, R. J. (1986), Secondary targets for the radiometric correction of AVHRR imagery for crop monitoring, *Proceedings of the Tenth Canadian Symposium on Remote Sensing*, Edmonton, Alberta, pp. 875–889.

McClatchey, R. A., Fenn, R. W., Selby, J. E., Volz, F. E., and Garing, J. S. (1971), Optical properties of the atmosphere, Report AFCRL-71-0279, Environmental Research Paper No. 354, AFCRL, Hanscom Field, Bedford, MA.

Price, J. C. (1987), Calibration of satellite radiometers and the comparison of vegetation indices, *Remote Sens. Environ.* 21:15–27.

Price, J. C. (1988a), An update on visible and near infrared calibration of satellite instruments, *Remote Sens. Environ.* 24:419–422.

Price, J. C. (1988b), Erratum—Calibration of the NOAA 10 AVHRR, *Remote Sens. Environ.* 26:303.

Slater, P. N., Biggar, S. F., Holm, R. G., Jackson, R. D., Mao, Y., Moran, M. S., Palmer, J. M., and Yuan, B. (1987), Reflectance- and radiance-based methods for the in-flight absolute calibration of multispectral sensors, *Remote Sens. Environ*, 22:11–37.

Smith, G. R., Levin, R. H., Koyanagi, R. S., and Wrigley, R. C. (1989), Calibration of the visible and near-infrared channels of the NOAA-9 AVHRR using high-altitude aircraft measurements from August 1985 and October 1986, NASA Technical Memorandum 101063, NASA Ames Research Center, Moffett Field, CA.

Tanré, D., Deroo, C., Duhaut, P., Herman, M., Morcrette, J. J., Perbos, J., and Deschamps, P. Y., (1985), Effets atmosphériques en télédétection - logiciel de simulation du signal satellitaire dans le spectre solaire, in *Proc. Third Int. Colloq. on Spectral Signatures of Objects in Remote Sensing*, ESA SP-247, pp. 315–319.

Tucker, C. J., Gatlin, J. A., and Schneider, S. R., (1984), Monitoring vegetation in the Nile Delta with NOAA-6 and NOAA-7 AVHRR imagery, *Photogramm. Eng. Remote Sens.* 50:53–62.